

# Inhibition of Localized Corrosion in 2205 Duplex Stainless Steel by Expired Myambutol (Ethambutol Hydrochloride) Drug in Acid Catalyzed Environment

<sup>1</sup> Benedict U. Ugi \*

<sup>1</sup>Department of Pure & Applied Chemistry  
University of Calabar, P. M. B. 1115  
Calabar, Nigeria

<sup>2</sup> Mbang E. Obeten

<sup>2</sup>Department of Chemistry  
Cross River University of Technology, P. M. B. 1123  
Calabar, Nigeria

**Abstract:-** Corrosion can be influenced by either the nature of the metal, nature of the environment (temperature, aeration, agitation or pH of the electrolyte) or the corrosion products. In order to minimize or completely eradicate their effects as a result of these influences on corrosion of 2205 duplex stainless steel, the corrosion inhibition performance of expired myambutol was studied in 0.5 M HCl environment at ambient temperature and elevated temperatures of 303, 313 and 333 K. The experimental and analysis work was carried out using both chemical and electrochemical techniques. Analytical results indicated that expired myambutol drug used as inhibitor adsorbed effectively on the surface of the 2205 duplex stainless steel hence inhibiting the factors influencing the corrosion of the steel. This was evident from the results of gravimetric, thermometric, EIS and Potentiodynamic polarization analysis recorded as 98.3 %, 98.5 %, 84.2 % and 91.9 % respectively. Generally inhibition efficiency increased with increased concentration of expired myambutol inhibitor but decreased with rise in temperature, an indication of initial strong adsorption of inhibitor and a subsequent dissolution of inhibitor from metal surface as a result of strong agitation from prolonged temperature effects. The physical adsorption process was attributed to the adsorption of inhibitor following the correlation coefficient values from the Langmuir profile drawn.

**Keywords:-** Myambutol, Adsorption, Corrosion, Electrochemical, Polarization, Duplex Stainless Steel, Inhibition Efficiency, Enthalpy.

## I. INTRODUCTION

The corrosion of stainless steel occurs primarily by electrochemical process involving oxidation and simultaneous reduction of some other species. The importance of corrosion studies is two folds. The first is economic, including the reduction of material losses resulting from the wasting away or sudden failure of

pipings, tanks, metal components of machines, ships, hulls, marine structures, etc (Abeng et al., 2018; Ade et al., 2014; Karthik and Sundaravachivelu, 2016; Karthikeyan, 2016). The second is conservation, applied primarily to metal resources, the world's supply of which is limited, and the wastage of which includes corresponding losses of energy and water resources accompanying the production and fabrication of metal structures. Awareness to corrosion and adaptation of timely and appropriate control measures hold the key in the abatement of corrosion failures. The important factors which may influence the corrosion process are: Nature of the metal, nature of the environment and the corrosion products, temperature, concentration of electrolyte, electrode potential, aeration, agitation and hydrogen over voltage and pH of the electrolyte (Karthikeyan, 2016; Ansari et al., 2017; Al-Amiery et al., 2014; Ali and Suleiman, 2018). To protect metals or alloy from corrosion, approaches such as isolating the structure from aggressive media of compensating for the loss of electrons from the corroded structure are employed. Corrosion inhibition may include organic or inorganic compounds that adsorb on the metallic structure to isolate it from its surrounding media to stop the oxidation-reduction process (Karthikeyan, 2016; Ansari et al., 2017; Al-Amiery et al., 2014). The action of drugs as inhibitors arises from their ability to treat metal and alloy surfaces consequent upon their addition in very low concentrations around corrosive environment. They are deemed to be rich, naturally synthesized chemical compounds that affect the corrosion rate by adsorption of effective species on metal surfaces when added to any industrial system through alteration of either anode or cathode reactions, formation of coating on metal through increased electrical resistance, etc. (Ade et al., 2014; Karthikeyan, 2016; Ansari et al., 2017; Al-Amiery et al., 2014; Ali and Suleiman, 2018). Stainless steel as a well-known metal of multi sectorial importance has its name connected to an entire group of iron-based metal which are the most commonly used metallic materials (Charles, 1991; Sanchez et al., 2002; IMO, 2014).

Element weight	% by
Cr	22.0 – 32.0
Ni	4.5 – 6.5 %
Mn	2.0 %
Si	1.0 %
P	0.03 %
S	0.02 %
C	0.03 %
N	0.1 – 0.2 %
Mo	3.0 – 5.0 %
Fe	Remaining

Table 1:- Chemical Composition of a Typical 2205 Duplex Stainless Steel in Weight Percent

Ethambutol is a medication primarily used to treat tuberculosis (Fig. 1). Ethambutol Hydrochloride is the hydrochloride salt form of ethambutol, an ethylenediamine derivative with antibacterial activity, specifically effective against mycobacteria (Lim, 2006). Although the exact mechanism of action of ethambutol hydrochloride is unknown, ethambutol hydrochloride inhibits the transfer of mycolic acids into the cell wall of bacteria, which impedes bacterial cell growth. This agent may also inhibit other cell metabolism, thereby preventing cell multiplication and causing cell death (Lim, 2006; Tripathi, 2015). Upon the bases that Myambutol, let alone its expired form has not be employed in the study of corrosion or corrosion related research, and the urgent need to minimize or completely eradicate 2205 duplex stainless steel corrosion effects in HCl environment at ambient and elevated temperatures prompted this research.

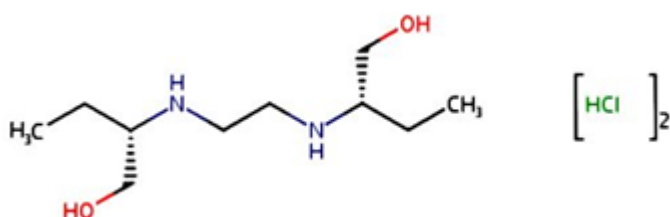


Fig 1:- Structure of (+)-2,2'-(Ethylenediimino)-di-1-butanol dihydrochloride ( $C_{10}H_{26}Cl_2N_2O_2$ )

## II. EXPERIMENTATION

### A. Preparation of Working Electrode (2205 Duplex Stainless Steel)

The working electrode (2205 duplex stainless steel) employed for this research work has the following composition (% by weight): Cr (22.0 – 32.0), Ni (4.5 – 6.5), Mn (2.0 max), Si Silicon (1.0 max), P (0.03 max), S (0.02 max), C Carbon (0.03 max), N (0.1 – 0.2), Mo (3.0 – 5.0) and Fe (Balance) respectively (Table 1). The electrode was resized to a dimension of 5cm x 4cm x 0.08cm for gravimetric analysis; 4cm x 0.08cm x 2.0cm for gasometric analysis and 1cm<sup>2</sup> x 1 cm<sup>2</sup> for the electrochemical measurements (electrochemical impedance spectroscopy and potentiodynamic polarization). The working electrode obtained from System Metals in Nigeria was carefully polished with different grades of emery paper to obtain a mirror surface, washed with distilled water, degreased with ethanol and rinsed in acetone and air dried then stored in a desiccators.

### B. Gravimetric Experimentation

Different concentration of inhibitor ranging from 500, 700, 1000, 1500 and 2500 ppm were used for the gravimetric experiment. Inhibitor solution of different concentrations were measured into a 100 ml beaker each where coupons were suspended in the solution for 5 hours of 1 hour each. After every 1 hour, the coupons were removed from the inhibitor solution and washed with distilled water, degreased with ethanol, rinsed in acetone and air dried, then reweighed. Data obtained from this experimental process were used to calculate the corrosion rate of the steel, the surface coverage and inhibition efficiency of the inhibitor following equations 1 and 2.

$$\theta = 1 - \frac{w_i}{w_o} \quad \dots(1)$$

$$IE \% = \left[ 1 - \frac{w_i}{w_o} \right] \times 100 \quad (2)$$

Where  $w_i$  and  $w_o$  explains values for weight loss with and without the inhibitors. Every of the reagent applied in this study was of analytical grade and all solutions were prepared using distilled water.

### C. Thermometric Experimentation

The thermometric technique which is a temperature dependent technique made use of a water bath which its temperature was regulated at every trial. The resized steel of dimension 4cm x 0.08cm x 2.0cm which was polished to a mirror surface was dropped into a beaker containing a blank solution (0.5 M HCl acid) and the beaker immersed in a water bath regulated to 313 K. after 60 minutes, the metal was removed, washed with distilled water, degreased with ethanol, rinsed in acetone and air-dried before weighing. This procedure was repeated for same blank at regulated temperatures of 323 and 333 K. The same experiment was conducted in the presence of Myambutol (Ethambutol hydrochloride) inhibitor at 500, 700, 1000, 1500 and 2500 ppm concentrations. The study

was conducted using a MEMMERT WNB – 14 thermostat water bath.

**D. Electrochemical Methods**

A three compartment electrochemical impedance cell was employed for this investigation with a saturated calomel (SCE) electrode as the reference electrode and a 1cm<sup>2</sup> platinum foil as a counter electrode. The working electrodes which was the 2205 duplex stainless steel with surface area of 0.28 cm<sup>2</sup> was dipped in 0.5 M HCl solutions. Electrochemical tests was conducted within a frequency of 10 Hz - 100,000 Hz within Potentiodynamic conditions, with an amplitude of 5 mV, involving alternating current signal at E<sub>corr</sub>. All experiments were conducted every 30 min with the inhibitor inclusive.

The inhibition efficiency which was determined from the values of the charge transfer resistance was calculated using Equation 3:

$$IE\% = \frac{R_{i_{ct}} - R_{o_{ct}}}{R_{i_{ct}}} \times 100 \dots \dots \dots 3$$

Where R<sup>i</sup><sub>ct</sub> and R<sup>o</sup><sub>ct</sub> represent the charge transfer resistance with and without the inhibitors. The behavior of stainless steel coupons with and without the extracts was investigated potentiodynamically by drawing up the anodic site and cathodic plots. Analysis was carried out on standard acid with varied partitions of inhibitor by altering the eV between -250 to + 250 mV following a scan rate of 1 mV/sec.

Corrosion current densities values were obtained using Equation 4:

$$IE\% = \frac{I_{o_{corr}} - I_{i_{corr}}}{I_{o_{corr}}} \times 100 \dots \dots (4)$$

Where I<sup>i</sup><sub>corr</sub> and I<sup>o</sup><sub>corr</sub> represent the corrosion current density with and without the inhibitor concentrations.

**III. RESULT AND DISCUSSION**

**A. Gravimetric Analysis and Results**

Upon immersion of 2205 Duplex Stainless steel coupon in the system containing the 0.5 M HCl acid after 5 hour, the rate of dissolution of the metal was noticed to be higher compared to the systems containing acid plus various concentrations of Myambutol (Ethambutol hydrochloride) inhibitor. This observation was similar to what was observed in the studies of corrosion by other researchers (Karthikeyan, 2016; Attari et al., 2017; Chidiebere et al., 2015; Guruprasad et al., 2018). It was confirmed that the steel dissolution was reducing with increasing concentration of the inhibitor as time progresses (Figure 2). The dissolution effect of the metal observed in the free acid solution was attributed to the strong action of the acid on the metal surface due to rapid hydrogen evolution (Chidiebere et al., 2015 ; Atheel et al., 2017; Lgaz et al., 2017; Ugi and Obeten, 2019). The gradual reduction in dissolution of the metal as inhibitor concentration was increased (Figure 3) could be explained on the bases of inhibition of the steel consequence upon replacement of the water molecule on the steel by inhibitor molecules (Abeng et al., 2018; Ade et al., 2014). This action could be seen from Table 2 as corrosion rate of the metal reduced, surface coverage and inhibition efficiency of the inhibitor increased with increase in concentration.

Conc. (g/L)	CR (mg/cm2/h)	θ	%IE
0.5 M HCl	1.119	-	-
500ppm	0.482	0.569	56.9
700ppm	0.271	0.758	75.8
1000ppm	0.103	0.908	90.8
1500ppm	0.094	0.916	91.6
2500ppm	0.019	0.983	98.3

Table 2:- 2205 Duplex Stainless Steel Corrosion Rate, Surface Coverage and % IE of Myambutol (Ethambutol hydrochloride) Inhibitor from Weight Loss in 1M HCl

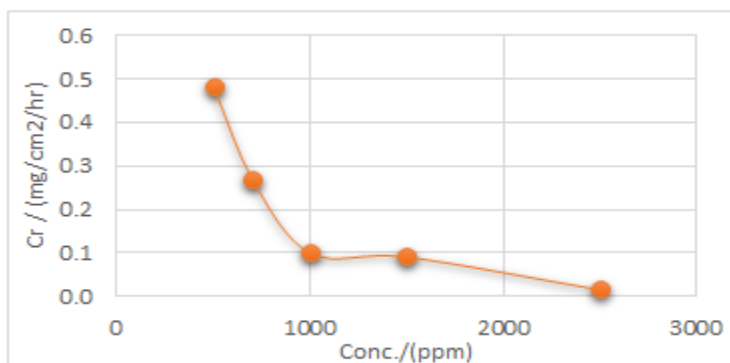


Fig 2:- Graphical Representation of the Variation of Corrosion Rate of Steel with Inhibitor Concentration at Ambient Temperature in 0.5 M HCl Environment

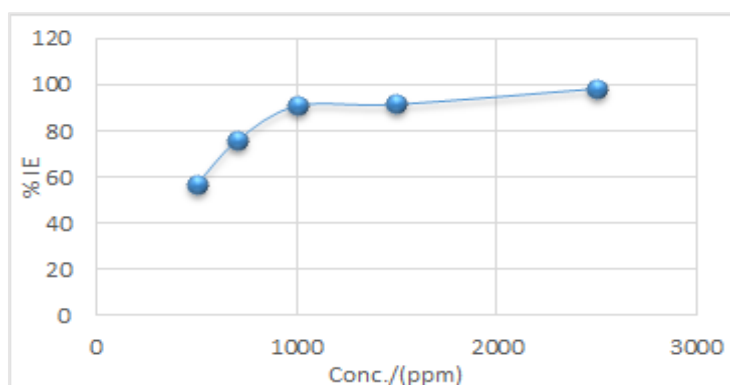


Fig 3:- Graphical Representation of the Variation of Inhibition Efficiency of Inhibitor with Inhibitor Concentration at Ambient Temperature in 0.5 M HCl Environment

**B. Thermometric Results and Analysis**

Thermometric analysis is temperature dependent and this method aid in accessing the effect of temperature on the inhibitor/steel interface. From Table 3, it can be observed that there is a gradual dissociation of the inhibitor molecules from the steel surface, consequence upon the agitation experienced by the system due to temperature increase. However, the result obtained still showed that the inhibitor had a significant adsorption adherence on the metal surface even at increasing temperature. The corrosion rate of the metal was seen to increase with increase in temperature which is explained on the bases of breaking of bonds between weak adsorbed inhibitor molecules and the

steel surface held by Van der Waals forces of attraction (Attari et al., 2017; Atheel et al., 2017; Swetha et al., 2018; Hebbar et al., 2018; Eddy et al., 2015). At each temperature, it was observed that the inhibition efficiency increased with increased inhibitor concentration and this could be explained from the fact that there is an increased surface coverage by the inhibitor and strong adsorption of greater inhibitor molecules that could not be easily affected by the temperature agitation (Abeng et al., 2018; Eddy et al., 2015; Jothi et al., 2017). The temperature effect on the inhibitor could also be explained as a physical adsorption process.

Conc. (ppm)	CR (mg/cm <sup>2</sup> /h)			θ			% IE		
	303K	313K	333K	303K	313K	333K	303K	313K	333K
0.5 M HCl	9.627	13.192	21.416	-	-	-	-	-	-
500	3.011	4.564	8.173	0.687	0.654	0.618	68.7	65.4	61.8
700	2.719	4.271	7.319	0.718	0.676	0.658	71.8	67.6	65.8
1000	1.397	2.382	5.101	0.855	0.819	0.762	85.5	81.9	76.2
1500	0.814	1.323	4.294	0.915	0.900	0.799	91.5	90.0	79.9
2500	0.142	0.624	2.065	0.985	0.953	0.904	98.5	95.3	90.4

Table 3:- Corrosion Rate of Steel, Surface Coverage and % IE of Expired Myambutol Inhibitor in 0.5 M HCl at 303, 313 and 333 K from Thermometric Experimentation.

C. Electrochemical Analysis and Results

Nyquist plots for duplex stainless steel in 0.5 M HCl solution in the presence and absence of different concentrations of Myambutol (Ethambutol hydrochloride) inhibitor is shown in Figs. 4. The plots obtained are similar to those in the absence of inhibitor consisting of high frequency capacitive loop which show that the impedance behaviour profile was unaltered by the change in inhibitor concentration, hence, a similar metal dissolution mechanism with and without the inhibitor (Oduote et al., 2016; Okewale and Olaitan, 2017; Adil, 2015; Olawale et

al., 2015; Olusegun et al., 2016). At all concentrations of the inhibitor, the duplex stainless steel was inhibited spontaneously especially on account of the fact that the charge transfer resistance exhibited its maximum inhibition efficiency for the duplex stainless steel at maximum concentration of 2500 ppm used for the research (Karthikeyan, 2016; Olawale et al., 2015; Olusegun et al., 2016 ; Ugi et al., 2016). The inhibition is associated with the adsorption of the inhibitor on the duplex stainless steel surface. The data for the electrochemical parameters obtained from the Nyquist plots are presented in Table 4.

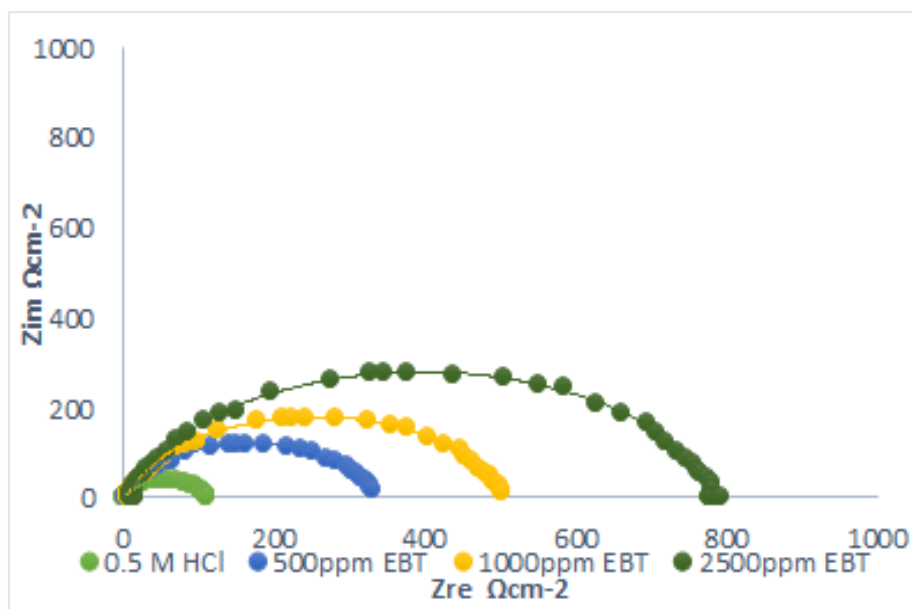


Fig 4:- Nyquist Plots for Duplex Stainless Steel at Ambient Temperature for Expired Myambutol Inhibitor in 0.5 M HCl Environment

Conc. (ppm)	$R_{ct}$ ( $\Omega\text{cm}^{-2}$ )	$\Theta$	% IE
0.5 M HCl	127	-	-
500	377	0.6631	66.3
1000	503	0.7475	74.8
2500	796	0.8405	84.2

Table 4:- EIS Data for Duplex Stainless Steel at Ambient Temperature for Expired Myambutol Inhibitor in 0.5 M HCl Environment

The corrosion kinetic parameters: corrosion potential ( $E_{corr}$ ) and corrosion current density ( $I_{corr}$ ) were obtained from the representative Tafel plots for duplex stainless steel in 0.5 M HCl solution in the absence and presence of different concentrations of the inhibitor (Fig. 5). The data for Corrosion potential, corrosion current density and inhibition efficiency is shown in Table 5. From Tables 5, it is observed that the values of  $I_{corr}$  decreased with steady increase in the inhibitor concentration. The inhibition efficiency result is an indication that Myambutol (Ethambutol hydrochloride) inhibitor showed more corrosion retardation on the alloy by adsorbing effectively

on the surface ( Guruprasad et al., 2018). Anodic shift in the values of  $E_{corr}$  was observed, suggesting that inhibitor acted as mixed inhibitor for on duplex stainless steel in 0.5 M HCl solutions (Tripathi, 2015) which of course is in agreement with the cathodic and anodic Tafel plots obtained. From the result obtained from the Tafel plots, it can be concluded that the extracts acted as mixed type inhibitors but acted majorly by retarding the rate of anodic dissolution than the cathodic hydrogen evolution for the coupon. Similar results had been reported from the inhibition of metals by plant extracts (Abeng et al., 2018, Atheel et al., 2017).

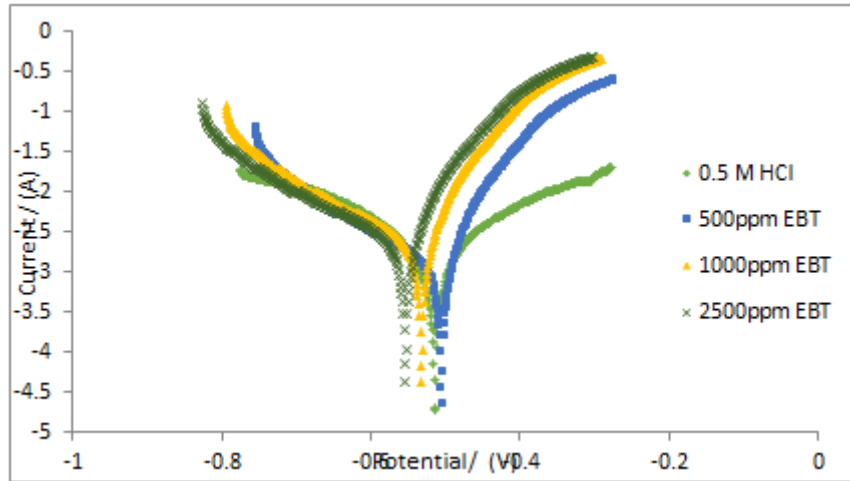


Fig 5:- Tafel Plots Showing Effect of Increasing Concentrations of Expired Myambutol Inhibitor on Duplex Stainless Steel at Ambient Temperature in 0.5 M HCl Environment

Conc. (ppm)	I <sub>corr</sub> (mAcm <sup>-2</sup> )	E <sub>corr</sub> (mV)	IEi (%)
0.5 M HCl	17.144	-194	-
500	6.796	-927	60.0
1000	2.085	-311	87.8
2500	1.391	-85	91.9

Table 5:- Potentiodynamic Polarization Parameters for Expired Myambutol Inhibitor on Duplex Stainless Steel at Ambient Temperature in 0.5 M HCl Environment

D. Thermodynamic Analysis

The standard free energy ( $\Delta G^{\circ}_{ads}$ ) for the adsorption of the Myambutol (Ethambutol hydrochloride) inhibitor was calculated using the Gibbs-Helmoltz (Equation 5 and 6).

$$k = \frac{1}{55.5} \exp \frac{-\Delta G^{\circ}_{ads}}{RT} \dots(5)$$

$$\Delta G^{\circ}_{ads} = - RT \ln(55.5 \times K_{ads}) \dots(6)$$

The adsorption free energy as a thermodynamic parameter in corrosion study was obtained from equilibrium constant derived out of the Langmuir isotherm plots. Values of this function are displayed in Fig. 8. A more negative value of  $\Delta G^{\circ}_{ads}$  is related to higher spontaneous reaction, i.e. higher corrosion rate (Lgaz et al., 2017; Swetha et al., 2018; Fouda et al., 2019). The negative free energy of adsorption ( $\Delta G^{\circ}_{ads}$ ) values in Fig. 8 revealed the spontaneous adsorption reaction process at low temperatures, and high stabled inhibition process (Al-Amiery et al., 2014; Attari et al., 2017; Ugi and Obeten, 2016 ). Physical adsorption mechanism is related to standard free energy of adsorption  $\Delta G^{\circ}_{ads}$  in aqueous solution (Eddy et al., 2015; Swetha et al., 2018; Abdel et al., 2015).

Arrhenius model gives the relationship between the corrosion rate and the minimum energy required before adsorption is activated according to Equations 7 and 8

$$C_r = A e^{\frac{-E_a}{RT}} \dots(7)$$

$$\ln C_r = \ln A - \frac{E_a}{RT} \dots(8)$$

Where  $C_r$  is the corrosion rate,  $E_a$  is the activation energy of the corrosion process,  $A$  is the pre-exponential factor,  $R$  is the gas constant and the  $T$  represent the absolute temperature. The plots is shown in Figure 6. Activation energy values were higher in the inhibited solution as compared to the blank, a projection of an adsorption effect. (Chidiebere at al., 2015; Okewale and Olaitan, 2017; Fouda et al., 2019). The pre-exponential factor also known as the frequency factor represents the frequency of collisions between reactant molecules, in this case the inhibitor molecules. The data in Table 6 shows more inhibition reaction as the concentration increases. This is explained on the bases of lesser acid reaction on the metal surface due to opportunity for increase inhibitor molecular collision (Al-Amiery et al., 2014; Hebbar et al., 2018; Abdallah et al., 2016; Abdel et al., 2015). A plot of  $\log (CR/T)$  versus  $1/T$  should be linear with slope equal to  $-(\Delta H^{\circ})/RT$  and intercept equal to  $[\log (R/Nh) + (\Delta S^{\circ})/R]$  from which the values of  $\Delta H$  and  $\Delta S$  are calculated according to the transition state Equation 9:

$$R_c = \frac{KT}{h} \exp\left(\frac{\Delta S^*}{R}\right) \exp\left(\frac{-\Delta H^*}{RT}\right) \dots(9)$$

The straight line  $\ln C_R/T$  vs.  $1/T$  is shown in Figs. 7. Table 6 revealed that the negative signs of enthalpy ( $\Delta H$ ) reflect the exothermic nature of dissolution process Paul and Machunda, 2016; Atheel et al., 2017; Ugi et al., 2016).

The values for entropy implies the decrease in disordering effect on going from reactants to the activation complex (Abeng et al., 2018; Ansari et al., 2017; Eddy et al., 2015; Kolo et al., 2018).

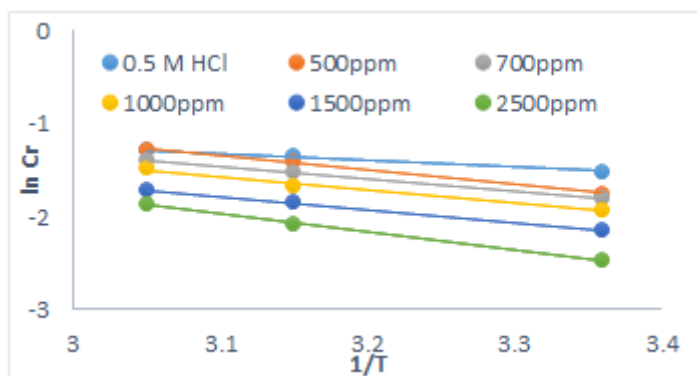


Fig 6:- Arrhenius Graph for the Adsorption of Expired Myambutol Inhibitor on Duplex Stainless Steel at Ambient Temperature in 0.5 M HCl Environment

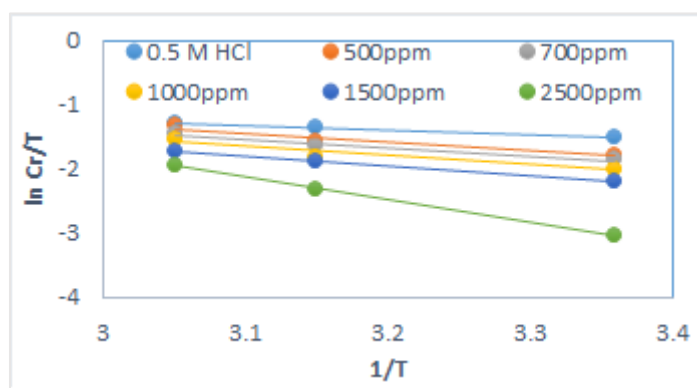


Fig 7:- The Transition State Plots for the Adsorption of Expired Myambutol Inhibitor on Duplex Stainless Steel at Ambient Temperature in 0.5 M HCl Environment

Conc. (ppm)	Ea	A	$\Delta H_{ads}$ kJ/mol	$\Delta S_{ads}$ kJ/mol
0.5 M HCl	7.6	1.01	-14.5	-162.2
500ppm	13.8	2.51	-18.3	-171.9
700ppm	14.9	2.71	-21.9	-193.4
1000ppm	16.0	2.73	-23.0	-201.5
1500ppm	19.3	3.39	-27.4	-213.9
2500ppm	20.1	3.96	-33.8	-237.0

Table 6:- Activation Energy and Thermodynamic Parameters for the Adsorption of Expired Myambutol Inhibitor on Duplex Stainless Steel at Ambient Temperature in 0.5 M HCl Environment

*E. Monolayer Adsorption Investigation*

In order to find out the nature of adsorption of the myambutol drug on the investigated surface, Equation 10 which is for Langmuir adsorption was approached. (Guruprasad et al., 2018; Adil et al., 2015).

$$\frac{c}{\theta} = \frac{1}{K} + C \quad \dots\dots(10)$$

The correlation coefficient values ( $R^2$ ) are approximately unity as shown in Fig. 8. This shows that the

data obtained for the inhibitor fits well to the Langmuir adsorption isotherm. Since it fits well to the adsorption isotherm, it therefore implies a monolayer adsorption of inhibitors (Eddy et al., 2015; Swetha et al., 2018). The values of equilibrium constant obtained from the intercept of the isotherm plots are seen to increase with increase in temperature suggesting that the inhibitors are physically adsorbed on the surface of the metal, and that the reaction is exothermic (Odusote et al., 2016).

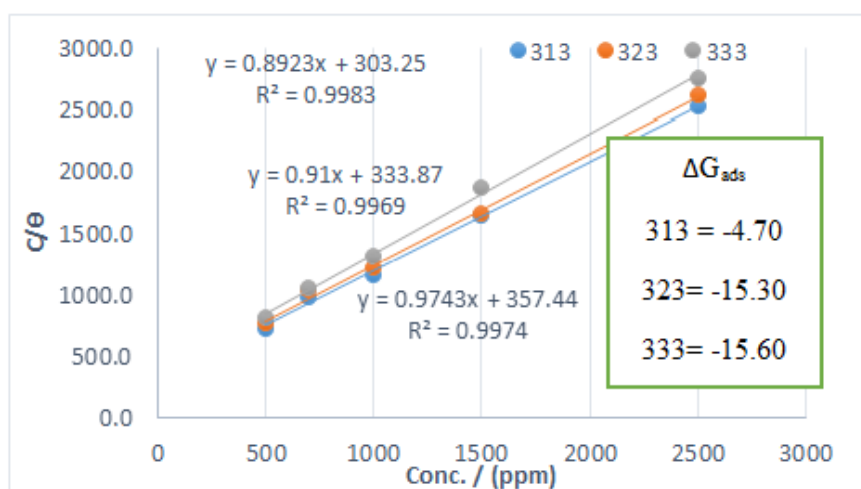


Fig 8:- Langmuir Isotherm for the Adsorption of Expired Myambutol Inhibitor on Duplex Stainless Steel at Ambient Temperature in 0.5 M HCl Environment

#### IV. CONCLUSION

The research findings drawn from the data analysis and results are as follows:

- Expired Myambutol (Ethanbutol Hydrochloride) proved an excellent inhibitor on 2205 duplex stainless steel in 0.5 M HCl environment. This was evident from the inhibition efficiency results obtained from gravimetric, thermometric, EIS and Potentiodynamic polarization analysis recorded at 98.3 %, 98.5 %, 84.2 % and 91.9 % respectively.
- Mechanism of adsorption points to physical adsorption of the expired Myambutol (Ethanbutol Hydrochloride) inhibitor on the steel surface. This was seen from the
- Anodic shift in the values of  $E_{corr}$  was observed, suggesting that inhibitor acted as mixed inhibitor on the duplex stainless steel in 0.5 M HCl solutions which of course is in agreement with the cathodic and anodic Tafel plots obtained.
- The values of equilibrium constant obtained from the intercept of the isotherm plots are seen to increase with increase in temperature suggesting that the inhibitors are physically adsorbed on the surface of the metal, and that the reaction is exothermic.
- Thermodynamic data obtained revealed that the expired Myambutol (Ethanbutol Hydrochloride) inhibitor was spontaneous, stable and physically adsorbed.

#### REFERENCES

- [1]. Abdel Hameed RS, Ismail EA, Abu-Nawwas AH, Al-Shafey HI. (2015) Expired voltaren drugs as corrosion inhibitor for aluminium in hydrochloric acid. *International Journal of Electrochemical Science*; 10:2098–2109
- [2]. Abeng FE, Idim VD. (2018). Green corrosion inhibitor for mild steel in 2 M HCl solution: Flavonoid extract of *Erigeron floribundus*. *World science news*; 9: 99
- [3]. Ade SB, Shitole NV, Lonkar SM. (2014). Antifungal drug's used as metal corrosion inhibitor in various acid medium. *Int J ChemTech Res*; 6(7):3642–3650
- [4]. Adil H. (2015). Corrosion inhibition of zinc metal in 2 M hydrochloric acid solution by using guaifenesin drug as an inhibitor and theoretical calculations. *J AlNahrain Univ*; 18(1):60–65
- [5]. Al-Amiery AA, Abdul A, Kadhum H, Kadhum A, Mohamad AB, How CK, Junaedi S. (2014). Inhibition of mild steel corrosion in sulfuric acid solution by new Schiff base. *Materials*; 7: 816.
- [6]. Ali IH, Suleiman HA. (2018). Effects of acid extract of leaves of *Juniperus procera* on corrosion inhibition of carbon steel in HCl solution. *Int J Electrochem Sci*; 13: 3922
- [7]. Atheel HA, Dhuha HF, Ali AA, Abdul Hameed F, Yousif E. (2017). Inhibitive effect of atenolol on the corrosion of zinc in hydrochloric acid. *Rasayan J Chem*; 10(3):922–928
- [8]. Attari HE, Chefira A, Elkihel A, Siniti M, Rehid H, Benabbouha T. (2017). Thermodynamics and electrochemical investigation of 2 – Mercaptobenzimidazole as corrosion inhibitors for mild steel C35E in hydrochloric acid solution. *Int J Sci Eng Investig*; 6: 143
- [9]. Charles J. (1991). Super duplex stainless steels: structure and properties. *Proceedings of Duplex Stainless Steels*. UK. p. 3
- [10]. Chidiebere MA, Oguzie EE, Liu L, Li Y, Wang F. (2015). Adsorption and corrosion inhibiting effect of riboflavin on Q235 mild steel corrosion in acidic environments. *Mater Chem Phys*; 156: 104
- [11]. Eddy NO, Momoh-Yahaya H, Oguzie EE. (2015). Theoretical and experimental studies on the corrosion inhibition potentials of some purines for aluminum in 0.1 M HCl. *J Adv Res*; 6(2): 217
- [12]. Guruprasad AM, Sachin HP, Swetha GA. (2018). Study of corrosion inhibition of mild steel by capacitabine in hydrochloric acid media. *Asian J Chem*; 30(7):1629–1633
- [13]. Hebbar N, Praveen BM, Prasanna BM, Sachin HP. (2018). Anticorrosion potential of flectofenine on mild

- steel in hydrochloric acid media: experimental and theoretical study. *J Fail Anal Prev.*; 1(11):371
- [14]. IMO. (2014). Practical guidelines for the fabrication of duplex stainless steel. International molybdenum association pub, London. p. 8
- [15]. Jothi RV, Maheshwari R, Saratha R, Vadivu DS. (2017). A study on inhibitive action of *Bauhinia racemosa* Lam. Extract as green corrosion inhibitor for mild steel in HCL medium, *Asian J Res Chem.*; 10(5): 615
- [16]. Karthikeyan S. (2016). Drugs/antibiotics as potential corrosion inhibitors for metals—a review. *Int J Chem Tech Res.*; 9(6):251–259
- [17]. Kolo AM, Idris S, Bamishaiye OM. (2018). Corrosion inhibition potential of ethanol extract of *Bryophyllum pinnatum* leaves for zinc in acidic medium. *Edelweiss Appl Sci Technol.*; 1(2):17–24
- [18]. Lgaz H, Salghi R, Jodeh S, Hammouti B. (2017). Effect of clozapine on inhibition of mild steel corrosion in 1.0 M HCl medium. *J Mol Liq.*; 225:271–280
- [19]. Lim SA. (2006). Ethambutol-associated optic neuropathy. *Ann. Acad. Med. Singapore*; 35(4): 274 – 278
- [20]. Odusote JK, Owalude DO, Olusegun SJ, Yahya RA. (2016). Inhibition efficiency of *Moringa oleifera* leaf extract on the corrosion of reinforced steel bar in HCl solution. *The West Indian J Engr.*; 38(2): 70
- [21]. Olawale O, Bello JO, Akinbami P. (2015). A study on corrosion inhibition of mild – steel in hydrochloric acid using cashew waster. *Int J Mod Eng Res.*; 2: 73
- [22]. Olesgun SJ, Okoronkwo EA, Okotete AE, Ajayi OA.(2016). Gravimetric and electrochemical studies of corrosion inhibition potential of acid and ethanol extract of siam weed on mild steel. *Leonardo J Sci.*; 9: 55.
- [23]. Peter A, Obot IB, Sharma SK. (2015). Use of natural gums as green corrosion inhibitors: an overview. *Int J Ind Chem.*; 6(3): 164.
- [24]. Sanchez R, Moreno I, Almagro J, Bottela J, Llovet X. (2002). Effects of composition and thermal history on the phase balance and element distribution of standard and modified duplex stainless steel. 4<sup>th</sup> stainless steel science and market congress. Conference proceedings, p. 11
- [25]. Swetha GA, Sachin HP, Guruprasad AM, Prasanna BM, Sudheer Kumar KH. (2018). Use of seroquel as an effective corrosion inhibitor for low carbon steel in 1 M HCl. *J Bio Tribo Corros.*; 4:57
- [26]. Tripathi KD. (2015). Essentials of medical pharmacology, 7<sup>th</sup> ed. Jaypee pub. India. p. 769
- [27]. Ugi BU, Obeten ME. (2019). Investigating the Anticorrosion Potentials of Expired Nevirapine Antiretroviral as Inhibitor of Potential Crude Oil Steel in Acidic Medium. *Int Res J Innov Engr Techno.*; 3(4): 50.
- [28]. Ugi BU, Obeten ME, Uwah IE, Okafor PC. (2016). Aluminium corrosion abatement using non toxic and eco-friendly organic inhibitors. *J. Global Ecology and Envir.*; 4(4): 242 - 252